Artificial Cytoskeletal Structures Within Enzymatically Active Bio-inorganic Protocells

*Ravinash Krishna Kumar, Mei Li, Sam N. Olof, Avinash J. Patil, and Stephen Mann**

The chemical construction of artificial cellular systems that mimic aspects of primitive metabolism and/or replication has significant potential in advancing new horizons in synthetic biology,[1] soft matter biotechnology[2] and origins of life research.[3] Currently, several different scenarios for assembling protocell models are being pursued.[4] In general, these are based on the entrapment of biomolecules, genes and biological machinery within the aqueous interior of various types of self-assembled micro-compartments such as phospholipid vesicles,[5] lipid membrane-bounded phase-partitioned aqueous polymer droplets,[6] polymer hydrogel capsules,[7] block copolymer vesicles,[8] inorganic membrane-bounded water droplets[9,10] and membrane-free peptide/nucleotide micro-droplets.[11,12] However, although there are numerous *in vitro* studies that aim to mimic the biological mechanisms of cytoskeletal assembly and organization,[13–16] *in situ* synthesis of artificial cytoskeletal-like structures within protocell models using small-molecule precursors has only been addressed very recently.[17] In this regard, we reported the encapsulation and enzyme-mediated self-assembly of functionalized amino acid molecules within the interior of phospholipid vesicles as a step towards a synthetic protocell endowed with cytoskeletal-like internal structure. By employing small-molecule and non-covalent interactions, a continuous supramolecular hydrogel of amino acid-based nanofilaments could be reversibly assembled and disassembled within the vesicles, thereby mimicking at a simple level cytoskeletal properties such as shape deformation and motility. Such an approach could offer pathways to alternative types of cytoskeletal networks, and provide insights into the origin of proto-cytoskeletal elements in early cells, based for example on the supramolecular assembly of a wide range of derivatized amino acids,[18] or mononucleotides such as 5′-guanosine monophosphate.[19]

The possibility of developing artificial protocells with physically structured micro-environments provides a step towards the construction of synthetic cell-like entities with soft, viscoelastic interiors that in principle can be re-modelled by processes of reversible non-covalent self-assembly. Under such conditions, it should be possible to mechanically and chemically manipulate the protocell interior such that internalized mechanisms involved for example with enzyme catalysis, RNA replication, shape deformation or self-reproduction of the compartment, are influenced by higher-order processes. Here we initiate this approach by constructing enzymatically active, semi-permeable bio-inorganic protocells capable of self-assembling a nanostructured hydrogel interior and undergoing small-molecule dephosphorylation reactions. We prepare the microscale compartments in the form of Pickering emulsions[20] that comprise a suspension of nanoparticle-stabilized water micro-droplets (colloidosomes) dispersed in oil. The semi-permeable inorganic membrane consists of 20–30 nm-sized amphiphilic silica nanoparticles, and is spontaneously assembled at the oil/water droplet interface.[21] Specifically, we demonstrate that the *in situ* assembly of a supramolecular hydrogel within the colloidosomes can be achieved by alkaline phosphatase (ALP)-mediated dephosphorylation of *N*-fluorenylmethylcarbonyl-tyrosine-(*O*)-phosphate (FMOC-TyrP) entrapped within the water droplets (Supporting Information, Scheme 1). We investigate the structural characteristics of the incarcerated *N*-fluorenylmethylcarbonyl-tyrosine (FMOC-Tyr) hydrogel, and highlight the effect of confinement on changes in the morphology and higher-order structure of the constituent amino acid-based nanofilaments compared with analogous materials prepared in bulk solution. We also determine the kinetics of nanofilament growth within the colloidosomes, and show that gel-sol transitions can be utilised to modulate the viscosity of the protocell interior, which in turn can be used to influence the enzyme-mediated dephosphorylation of the small-molecule substrate, *p*-nitrophenylphosphate (*p*NPP).

A Pickering emulsion was prepared by the addition of surface-modified silica nanoparticles to a water/dodecane mixture with an aqueous/oil volume fraction of 0.033. Self-assembly of a viscoelastic supramolecular hydrogel within the colloidosomes was achieved by incorporating ALP and FMOC-TyrP within the entrapped aqueous phase, and ageing

R. Krishna Kumar, Dr. M. Li, S. N. Olof,
Dr. A. J. Patil, Prof. S. Mann
Centre for Organized Matter Chemistry
School of Chemistry
University of Bristol
Bristol, BS8 1TS, UK
E-mail: s.mann@bristol.ac.uk

S. N. Olof
Bristol Centre for Functional Nanomaterials
Centre for NSQI
University of Bristol
BS8 1FD, UK

DOI: 10.1002/smll.201201539

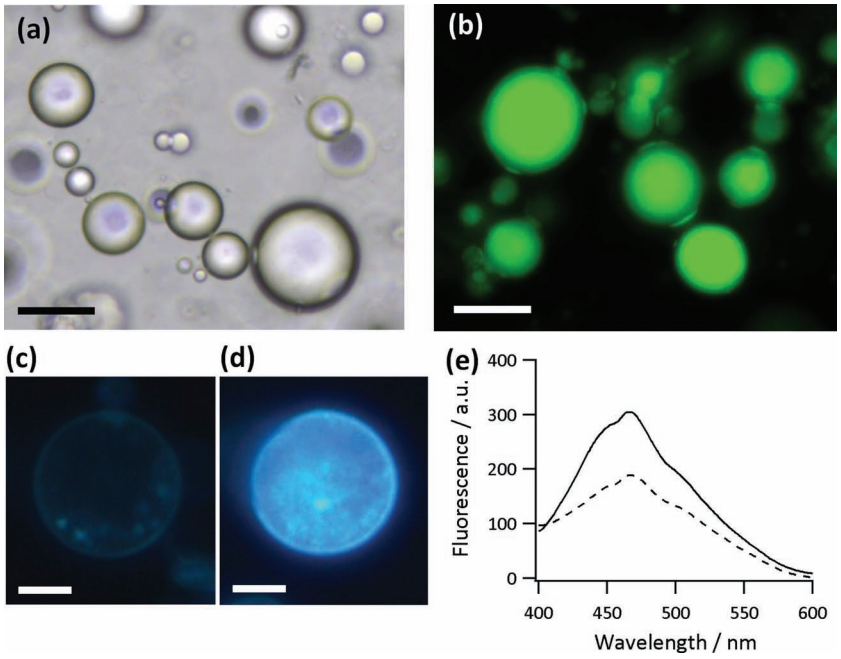

Figure 1. a) Optical micrograph of discrete spherical supramolecular hydrogel colloidosomes; scale bar = 50 μm. b) Fluorescence optical micrograph of calcein-encapsulated supramolecular hydrogel colloidosomes; scale bar = 50 μm. c,d) Fluorescence optical micrographs of single colloidosomes containing Hoechst 33258 prior to *in situ* nanofilament formation (c), and after 1 day showing nanofilament formation and extensive hydrogelation (d); (scale bars = 20 μm). e) Corresponding fluorescence spectra recorded for colloidosomes shown in (c) (dashed line) and (d) (solid line); the increase in intensity at 461 nm is consistent with strong binding of the dye to FMOC-Tyr nanofilaments assembled in the micro-compartment.

for 1 day (see Experimental methods). The dispersions partitioned into a turbid water-in-oil Pickering emulsion phase overlaid with a continuous oil phase. Optical images of the aged emulsion phase showed a suspension of well-defined spherical micro-compartments, 40 μm (σ = 17.3 μm) in size (**Figure 1**a,b; Supporting Information, Figure S1a), which were visually analogous to colloidosomes prepared in the absence of a hydrogelation reaction. However, whereas the latter were extensively fragmented on air drying, the dried hydrogel-filled colloidosomes appeared discrete and more translucent, consistent with a considerable increase in their mechanical stability (Supporting Information, Figure S1b,c). The presence of a hydrogel matrix throughout the silica nanoparticle-stabilized droplets was confirmed by fluorescence optical micrographs and complementary fluorescence spectroscopy measurements of individual colloidosomes containing the fluorescent dye, Hoechst 33258, which displayed a strong blue fluorescence in the presence of FMOC-Tyr nanofilaments (Figure 1c–e; Supporting Information, Figure S2).

Atomic force microscopy (AFM) and transmission electron microscopy (TEM) were used respectively to elucidate the structure of the inorganic membrane and hydrogel interior of the bio-inorganic protocells. AFM images of partially dried membrane fragments showed thin sheets, 52 nm (σ = 12 nm) in thickness that consisted of a closely packed array of nanoparticles with interparticle voids (Supporting Information, Figure S3). Similar observations were also made by TEM on partially disrupted colloidosomes. In addition, the negatively stained TEM images showed the presence of spheroidal hydrogel particles that were associated with the silica nanoparticles, and which comprised an entangled matrix of self-assembled nanofilaments (**Figure 2**a). The FMOC-Tyr filaments, which were 50 nm (σ = 14 nm) in width, were significantly wider than those formed in hydrogels prepared in bulk solutions (14 nm; σ = 3.5 nm) (Supporting Information, Figure S4) under identical reaction conditions. The increase in width was attributed to superstructure formation based on the co-aligned bundling of 5 nm-thick primary nanofilaments to produce well-ordered twisted fibril tapes within the protocell interior (Figure 2b).

Fluorescence spectra of colloidosome-entrapped or bulk solutions of FMOC-TyrP and ALP prior to hydrogelation showed a characteristic peak with a maximum at 313 nm and a broad shoulder from 350-400 nm (Supporting Information Figure S5). In both reaction systems, enzyme-mediated formation of FMOC-Tyr and subsequent nanofilament self-assembly resulted in a red-shift of the peak maximum and disappearance of the broad shoulder (**Figure 3**a, Supporting Information Figure S5). This was coupled with a considerable increase in intensity due to the presence of dominant excimer species and higher-order aggregates indicative of a monomer to nanofilament transformation.[22] Time-dependent changes in the bathochomic shift of the peak maximum were used to measure the kinetics of supramolecular assembly and provide quantitative comparisons between FMOC-Tyr self-assembly in bulk solution and within the protocell interior (Figure 3b,c; see Supporting Information). Enzyme-mediated nanofilament growth in solution followed typical sigmoidal kinetic curves with an initial nucleation lag phase (τ_{lag}) of 1.72 ± 0.50 h followed by a maximal nanofilament growth rate (v_{max}) of $7.8 \times 10^{-3} \pm 1.54 \times 10^{-10}$ Δnm mM^{-1} h^{-1} (Figure 3d).[23] In contrast, ALP-catalysed nanofilament growth within the colloidosomes displayed a convex rate profile with an increased maximal growth rate of $4.93 \times 10^{-1} \pm 2.79 \times 10^{-6}$ Δnm mM^{-1} h^{-1} without an apparent lag phase (Figure 3e).[23,24] The striking disappearance of the nucleation induction time and sixty-fold increase in v_{max} was consistent with complementary fluorescence microscopy images that monitored binding of Hoechst 33258 to the growing FMOC-Tyr filaments over time (Figure 3f,g). Fluorescence line intensity profiles of Hoechst 33258 binding recorded 0.25 h after colloidosome formation indicated that nucleation and initial growth of the supramolecular assemblies occurred preferentially at the internal surface of the silica nanoparticle membrane, followed by relatively fast growth of the hydrogel matrix towards the centre of the bio-inorganic protocell (Figure 3g). Previous studies on enzyme-mediated hydrogelation in bulk solution have shown that nucleation and early-stage nanofilament growth are spatially located at the site of enzyme action,[25]

small NANO MICRO

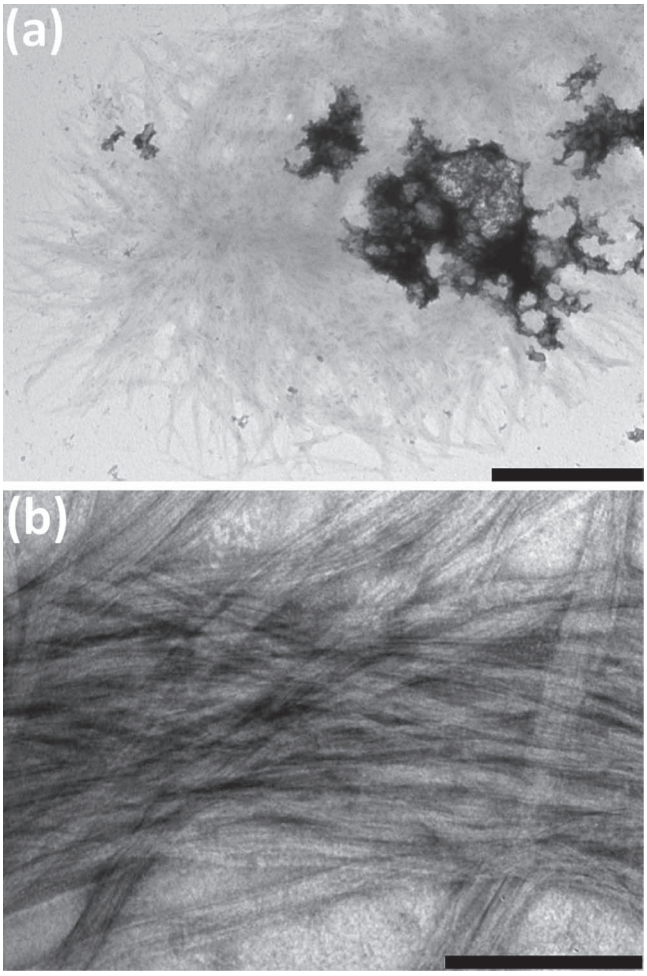

Figure 2. a) Low magnification TEM image of a disrupted single colloidosome showing confined matrix of FMOC-Tyr nanofilaments. A remnant of the silica nanoparticle membrane is attached to part of the supramolecular hydrogel.; scale bar = 1 μm. b) High magnification negatively stained image showing superstructural bundling of 5 nm-wide primary filaments into twisted tapes approximately 50 nm in thickness; scale bar = 200 nm.

suggesting that adsorption of ALP onto the inner wall of the silica nanoparticle membrane provides a high local enzyme concentration that is responsible for the increased rates of heterogeneous nucleation and growth in the bio-inorganic protocell. In contrast, the activation energy barrier to homogenous nucleation appeared to be a key factor responsible for the reduced kinetics of nanofilament formation in bulk solution. Moreover, molecular crowding and immobilization of ALP on the silica nanoparticle membrane could result in increased catalytic cooperativity,[26–28] which would in turn reduce the number of discontinuities between the nanofilaments and result in the bundled superstructures observed by TEM. Compared with nanofilament assembly in free solution, the faster rate of growth within the colloidosome interior could originate from the increased level of supramolecular crowding in the confined micro-environment, which provides many more sites for secondary nucleation. Although it was difficult to confirm this due to experimental challenges in measuring directly the length of the FMOC-Tyr nanofilaments, the larger red-shift (Δ = 5 nm) in the peak maximum associated with hydrogelation in bulk solution compared with that inside the colloidosomes (Δ = 2 nm) was consistent with the growth of shorter nanostructures within the bio-inorganic protocell.

Significantly, the hydrogel core of the nanoparticle-stabilized spherical microstructures could be disassembled by increasing the temperature to the gel-sol transition temperature of 45 °C, as determined by differential scanning calorimetry. Disassembly of the encapsulated hydrogel was monitored through the corresponding decrease in Hoechst 33258 fluorescence intensity associated with nanofilament disintegration and concomitant release of the bound dye molecules; cooling of the samples to room temperature re-assembled the hydrogel within the protocell interior (**Figure 4**a,b). These results indicated that the internal viscosity of the colloidosomes could be modulated by controlling the non-covalent interactions between the FMOC-Tyr molecular building blocks. As a consequence, we measured the viscosity of the hydrogel core, and then exploited temperature-induced changes in the viscosity to modulate ALP-mediated dephosphorylation of an auxiliary substrate molecule.

The viscosity of the nanoparticle-stabilized water droplets in the presence or absence of a spatially confined supramolecular hydrogel was determined by particle tracking of 2–3 μm-diameter silica beads encapsulated within the colloidosomes (see Supporting Information and Figure S6). The average viscosity (η) of the supramolecular hydrogel core of the protocells was 0.41 ± 0.17 Pa s with a corresponding diffusion constant (D) of $5.56 \times 10^{-16} \pm 1.50 \times 10^{-16}$ m^2 s^{-1}. This was approximately 100 times greater than the internal viscosity of aqueous-filled colloidosomes ($\eta = 0.0044 \pm 0.0021$ Pa s, $D = 4.52 \times 10^{-14} \pm 1.15 \times 10^{-14}$ m^2 s^{-1}), which was similar in magnitude to the viscosity of water (0.001 Pa s).

To determine the influence of changes of the viscosity on enzyme activity, we prepared colloidosomes as above comprising a FMOC-Tyr hydrogel core with embedded ALP molecules, and then added the substrate (*p*NPP) to the oil phase of the Pickering emulsion, and measured the dephosphorylation activity of the trapped enzyme at 30 or 45 °C (see Supporting Information). At both temperatures, a strong yellow colour associated with the formation of the highly water soluble product, *p*-nitrophenol (*p*NP) was observed specifically in the colloidosome phase within 15 mins of adding the substrate to the oil (Supporting Information, Figure S7). The observations confirmed that the silica nanoparticle membrane was sufficiently permeable for phase transfer of *p*NPP, and that the entrapped ALP molecules remained enzymatically active at 30 and 45 °C. Non-linear curve fitting was employed to determine the dependence of initial velocities (v_o) on substrate concentration (S), and in accordance with Michaelis-Menton kinetics, these data sets were used to calculate the maximum velocity (V_{max}) and Michaelis constant (K_m) (Figure 4c, and Supporting Information, Figure S8). The values of V_{max} and K_m were 3.77 mM min^{-1} and 4.29 mM, or 8.31 mM min^{-1} and 1.33 mM at 30 or 45 °C, respectively. The lower V_{max} at 30 °C was associated with a two-fold decrease in the turnover number (k_{cat}) of 2.17×10^4 s^{-1}

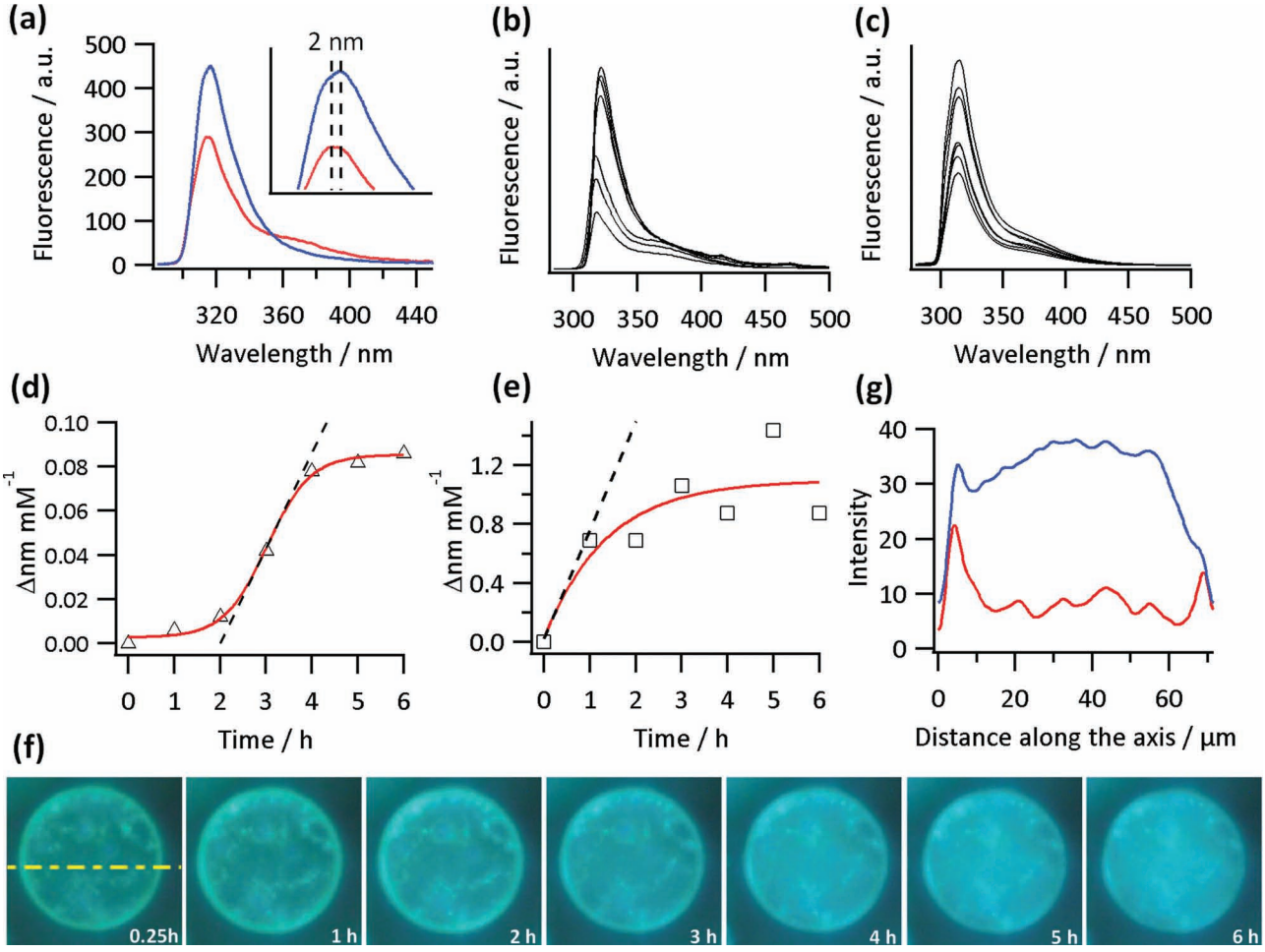

Figure 3. a) Fluorescence spectra of colloidosome-encapsulated FMOC-TyrP (red), and after ALP-mediated formation of encapsulated FMOC-Tyr nanofilaments (blue); a 2 nm red-shift in the peak maximum is observed (inset). b,c) Fluorescence spectra of solutions of FMOC-TyrP and ALP in bulk medium (b) or within colloidosomes (c) monitored over 6 h showing time-dependent increase in intensity and associated red shift. d,e) Plots showing kinetics of nanofilament growth over 6 h in bulk solution (d) or within colloidosmes (e). (f) Time-dependent fluorescence microscopy images showing *in situ* growth of FMOC-Tyr nanofilaments within a single colloidosome. Fluorescence emission is observed upon Hoechst 33258 binding to the growing nanofilaments. The size of the colloidosome is 70 µm. g) Corresponding fluorescence line intensity profiles of the colloidosome shown in (f) after 0.25 h (red) and 6 h (blue). The dye intensity is initially concentrated at the membrane surface (red profile) and develops to give a more homogenous intensity profile after 6 h (blue profile).

compared to 4.78×10^4 s^{-1} at 45 °C. Significantly, the catalytic efficiency (k_{cat}/K_m) improved seven-fold from 5.05×10^6 M^{-1} s^{-1} to 3.59×10^7 M^{-1} s^{-1} as the temperature was changed from 30 to 45 °C; that is, as the internal viscosity decreased by almost hundred-fold from approximately 0.4 to 0.004 Pa s. The decrease in turnover number and catalytic efficiency of ALP in the presence of an entangled network of confined FMOC-Tyr nanofilaments at 30 °C was attributed primarily to diffusional constraints associated with an increase in the internal viscosity of the micro-compartment rather than a reduction in the temperature of the reaction system. This was consistent with previous studies on lipase activity in colloidosomes with or without an agorose gel network,[10] as well as control experiments on *p*NPP dephosphorylation undertaken at 30 °C using aqueous-filled ALP-containing colloidosomes, which showed increased kinetic parameters (k_{cat} = 3.37 × 10^4 s^{-1}, k_{cat}/K_m = 2.03 × 10^7 M^{-1} s^{-1}) compared with the hydrogel-filled protocells. In addition, measurements of the catalytic efficiency of ALP-mediated *p*NPP dephosphorylation in bulk solution and in the absence of a FMOC-Tyr hydrogel did not change significantly between 30 and 45 °C (k_{cat}/K_m = 2.57×10^6 and 2.22×10^6 M^{-1} s^{-1}, respectively). We attributed the sixteen-fold higher catalytic efficiency determined at 45 °C for the colloidosome system (3.59×10^7 M^{-1} s^{-1}) compared with the reaction in bulk solution at the same temperature (2.22×10^6 M^{-1} s^{-1}) to the increased interfacial area available for mass transfer in the compartmentalized media.[9,10]

In conclusion, the spontaneous self-assembly of amphiphilic silica nanoparticles at the oil/water droplet interface provides a facile route to the construction of semi-permeable inorganic-based protocells capable of undergoing ALP-mediated dephosphorylation reactions in the presence of small-molecule substrates located within or external to the compartmentalized medium. *In situ* -assembly of an amino acid-based supramolecular hydrogel within the colloidosomes is used to generate an artificial cytoskeletal-like environment

small NANO MICRO

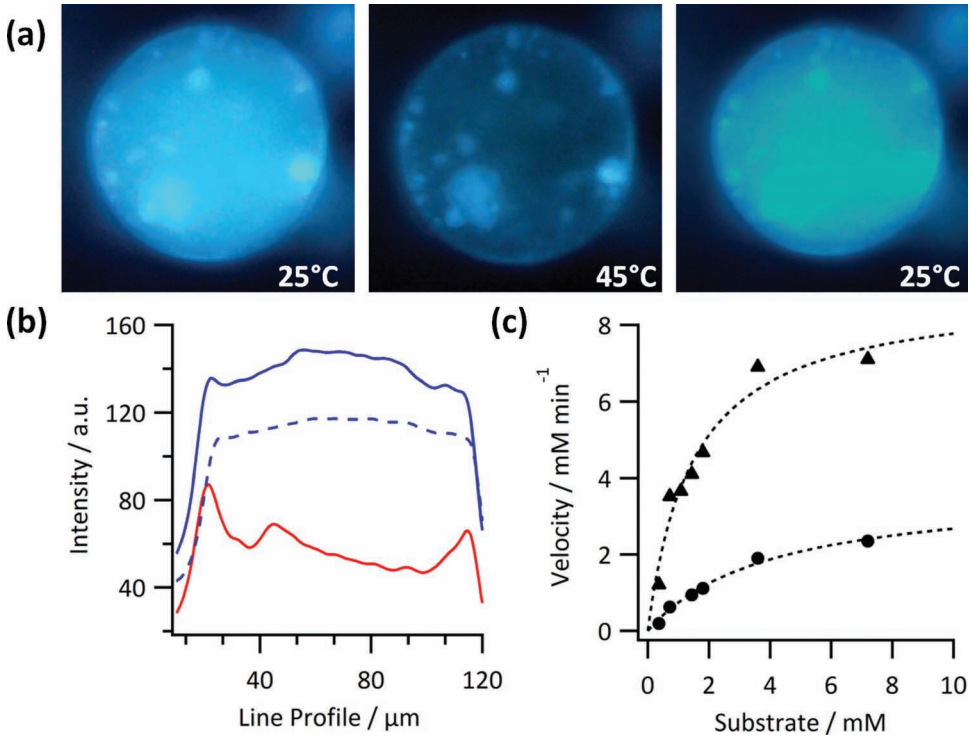

Figure 4. a) Fluorescence optical microscopy images of a hydrogel-containing colloidosome containing Hoechst 33258 at room temperature (left panel), at the gel-sol transition temperature (45 °C) after 5 min (middle panel) and subsequently cooled to room temperature after 30 min (right panel), illustrating disassembly and reassembly of nanofilaments within a colloidosome. b) Corresponding fluorescent line intensity profile of images shown in (a) at room temperature (blue trace), at 45 °C (red trace) and after cooling to room temperature (blue dashed trace). c) Enzyme kinetic plots for ALP-mediated dephosphorylation showing changes in initial velocities with substrate (*p*NPP) concentration for reactions undertaken in colloidosomes containing a hydrogel core (30 °C, circles) or a disassembled FMOC-Tyr hydrogel interior (45 °C, triangles).

comprising an entangled matrix of FMOC-Tyr nanofilaments and immobilized enzyme molecules. Nucleation of the amino acid-based nanofilaments occurs preferentially on the inner surface of the inorganic membrane, presumably due to surface adsorption of ALP molecules on the silica nanoparticles, and subsequent growth of the hydrogel is influenced by confinement and crowding effects associated with the protocell interior. Moreover, reversible disassembly of the supramolecular matrix at the gel-sol transition temperature results in a 100-fold decrease in the viscosity of the internalized environment, which in turn increases the turnover number and catalytic efficiency of the protocells. Finally, our results suggest that artificial protocells based on the integration of biological and inorganic nanoscale components could have significant potential in areas such bionanotechnology and synthetic biology. The chemical construction of such systems could also serve as an alternative model for evaluating potential pathways to minimal cell-like entities capable of physically and chemically organizing their internalized environments. As such, inorganic-based protocells could be useful models in origins of life research.[29,30]

Experimental Section

Preparation and Characterisation of FMOC-Tyrosine Supramolecular Hydrogel Colloidosomes: Partially hydrophobic silica nanoparticles with average diameters of 20–30 nm were prepared as described previously.[31] In brief, hydrophobic silica nanoparticles were silylated by reaction with dichlorodimethylsilane in the presence of water, followed by drying at 300 °C for 2 h to produce hydrophilic/hydrophobic nanoparticles comprising approximately 50% silanol ($-O_3SiOH$) and 50% dimethylsilane ($-O_2Si(CH_3)_2$) surface-functionalized groups. The preparation of silica nanoparticle colloidosomes comprising supramolecular hydrogel interiors was based on a reported procedure,[9,21] but with the following modifications. 10 µmol of *N*-fluorenylmethylcarbonyl-tyrosine-(*O*)-phosphate (FMOC-TyrP, Nova-biochem) was dissolved in 200 µL of an alkaline buffer (pH 10.3) containing 50 mM tris(hydroxymethyl)-aminomethane-HCl (Sigma), 50 mM sodium carbonate (Sigma), and 1 mM magnesium chloride (Sigma). The final pH of the solution was 7.8. Calf intestine alkaline phosphatase (ALP; 10 µL, Calbiochem, 1000 U mL^{-1}) was added, and 100 µL of the enzyme-containing solution mixed by gentle rotation with 30 mg of 50:50 hydrophillic/hydrophobic silica nanoparticles. (In other experiments, 100 µM of the water soluble fluorescent dyes, calcein (Sigma) or Hoechst 33258 (Sigma), and/or 1 µL of fluorescent silica beads (Corpuscular) were added to the aqueous reaction mixture). 3 mL of anhydrous dodecane (Sigma) was then added, followed by vigorous shaking for 1 minute to ensure complete emulsification. The volume fraction of water to oil was fixed at 0.033, and the amount of silica nanoparticles used was 0.3 mg μL^{-1} of the aqueous phase. In most experiments, colloidosomes containing encapsulated FMOC-TyrP and ALP were aged for at

least 1 day to ensure complete hydrogelation of the FMOC-Tyr nanofilaments.

Acknowledgements

We thank Prof. B. P. Binks for the gift of silica nanoparticles, Dr Stuart Bellamy for guidance with enzyme kinetics, Dr Andy Collins for help with AFM, the Bristol Centre for Nanoscience and Quantum Information for providing facilities, and EPSRC, the Bristol Centre for Functional Nanomaterials (Grant EP/G036780/1) and ERC (Advanced Grant scheme) for financial support.

[1] J. W. Szostak, D. P. Bartel, P. L. Luisi, *Nature* **2001**, *409*, 387.
[2] P. Stano, P. Carrara, Y. Kuruma, T. Souza, P. L. Luisi, *J. Mater. Chem.* **2011**, *21*, 18887.
[3] a) S. Mann, *Acc. Chem. Res.* DOI: 10.1021/ar200281t; b) S. S. Mansy, J. P. Schum, M. Krishnamurthy, S. Tobe, D. A. Treco, J. W. Szostak, *Nature* **2008**, *454*, 122; c) P. L. Luisi, F. Ferri, P. Stano, *Naturwissenschaften* **2006**, *93*, 1.
[4] A. J. Dzieciol, S. Mann, *Chem. Soc. Rev.* **2012**, *41*, 79.
[5] a) P. Stano, P. L. Luisi, *Chem. Commun.* **2010**, *46*, 3639; b) H. Kita, T. Matsuura, T. Sunami, K. Hosoda, N. Ichihashi, K. Tsukada, I. Urabe, T. Yomo, *ChemBioChem* **2008**, *9*, 2403.
[6] M. Andes-Koback, C. D. Keating, *J. Am. Chem. Soc.* **2011**, *133*, 9545.
[7] B. Städler, A. D. Price, R. Chandrawati, L. Hosta-Rigau, A. N. Zelikin, F. Caruso, *Nanoscale* **2009**, *1*, 68.
[8] R. J. R. W. Peters, I. Louzao, J. C. M. van Hest, *Chem. Sci.* **2012**, *3*, 335.
[9] M. Li, D. C. Green, J. L. R. Anderson, B. P. Binks, S. Mann, *Chem. Sci.* **2011**, *2*, 1739.
[10] C. Wu, S. Bai, M. B. Ansorge-Schumacher, D. Wang, *Adv. Mater.* **2011**, *23*, 5694.
[11] S. Koga, D. S. Williams, A. W. Perriman, S. Mann, *Nature Chem.* **2011**, *3*, 720.
[12] D. S. Williams, S. Koga, C. R. C. Hak, A. Majrekar, A. J. Patil, A. W. Perriman, S. Mann, *Soft Matter* **2012**, *8*, 6004.
[13] M. L. Gardel, J. H. Shin, F. C. MacKintosh, L. Mahadevan, P. Matsudaira, D. A. Weitz, *Science* **2004**, *304*, 1301.
[14] L.-L. Pontani, J. van der Gucht, G. Salbreux, J. Heuvingh, J.-F. Joanny, C. Sykes, *Biophys. J.* **2009**, *96*, 192.
[15] D. K. Fygenson, M. Elbaum, B. Shaiman, A. Libchaber, *Phys. Rev. E* **1997**, *55*, 850.
[16] L. Limozin, E. Sackmann, *Phys. Rev. Lett.* **2002**, *89*, 14.
[17] R. Krishna Kumar, X. Yu, A. J. Patil, M. Li, S. Mann, *Angew. Chem. Int. Ed.* **2011**, *50*, 9343.
[18] Z. Yang, G. Liang, B. Xu, *Acc. Chem. Res.* **2008**, *41*, 315.
[19] J. Dash, A. J. Patil, R. N. Das, F. L. Dowdall, S. Mann, *Soft Matter* **2011**, *7*, 8120.
[20] A. D. Dinsmore, M. F. Hsu, M. G. Nikolaides, M. Marquez, A. R. Bausch, D. A. Weitz, *Science* **2002**, *298*, 1006.
[21] B. P. Binks, R. Murakami, *Nature Mater.* **2006**, *5*, 865.
[22] K. Thornton, A. M. Smith, C. L. R. Merry, R. V. Ulijn, *Biochem. Soc. Trans.* **2009**, *37*, 660.
[23] J. T. Jerrett, P. T. Lansbury, *Cell* **1993**, *73*, 1055.
[24] T. P. J. Knowles, C. A. Waudby, G. L. Devlin, S. I. A. Cohen, A. Aguzzi, M. Vendruscolo, E. M. Terentjev, M. E. Welland, C. M. Dobson, *Science* **2009**, *326*, 1533.
[25] A. R. Hirst, S. Roy, M. Arora, A. K. Das, N. Hodson, P. Murray, S. Marshall, N. Javid, J. Sefcik, J. Boekhoven, J. H. van Esch, S. Santabarbara, N. T. Hunt, R. V. Ulijn, *Nature Chem.* **2010**, *2*, 1089.
[26] A. P. Minton, *J. Biol. Chem.* **2001**, *276*, 10577.
[27] R. Hancock, *J. Struct. Biol.* **2004**, *146*, 281.
[28] A. P. Minton, *J. Cell Sci.* **2006**, *119*, 2863.
[29] G. J. T. Cooper, P. J. Kitson, R. Winter, M. Zagnoni, D.-L. Long, L. Cronin, *Angew. Chem. Int. Ed.* **2011**, *50*, 10373.
[30] H. Birch, *Chem. World* **2012**, *9*, 44.
[31] S. Arditty, C. P. Whitby, B. P. Binks, V. Schmitt, F. Leal-Calderon, *Eur. Phys. J.* **2003**, *11*, 273.
[32] A. Jesorka, M. Markström, M. Karlsson, O. Orwar, *J. Phys. Chem. B.* **2005**, *109*, 14759.

Received: July 3, 2012
Revised: August 27, 2012
Published online: October 2, 2012